THE JOURNAL OF PHYSICAL CHEMISTRY A

 VOLUME 106, NUMBER 23, JUNE 13, 2002

FEATURE ARTICLE

$C + C_2H_2$: A Key Reaction in Interstellar Chemistry

David C. Clary,*,† Erasmo Buonomo,† Ian R. Sims,‡ Ian W. M. Smith,‡ Wolf D. Geppert,§ Christian Naulin,§ Michel Costes,§ Laura Cartechini,|| and Piergiorgio Casavecchia||

Department of Chemistry, University College London, 20 Gordon Street, London WC1H OAJ, U.K., School of Chemical Sciences, The University of Birmingham, Edgbaston, Birmingham B15 2TT, U.K., UMR 5803 CNRS - Université Bordeaux 1, Laboratoire de Physico-Chimie Moléculaire, Université Bordeaux 1, 33405 Talence Cedex, France, and Dipartimento di Chimica, Università di Perugia, 06123 Perugia, Italy

Received: January 31, 2002

The fast reaction between $C(^3P)$ and C_2H_2 is thought to be an important process in dense interstellar clouds as it provides a mechanism for the growth of carbon chains. This feature article describes a complementary series of recent experimental and theoretical investigations on this reaction. This includes kinetic measurements of rate constants at low temperatures and crossed molecular beam determinations of integral and differential cross sections. The theory employs first-principles electronic structure computations and wave packet dynamics to calculate cross sections and rate constants for forming the linear and cyclic isomers of C_3H which can be formed in the reaction. The rate constant and cross section measurements show that there are no barriers in the potential surface for the reaction, whereas the differential cross section experiments provide new evidence for the formation of $C_3 + H_2$ products. The theoretical results of overall rate constants and cross sections agree quite well with the experiments, and it is predicted that the linear isomer of C_3H should be formed preferentially at low temperatures.

I. Introduction

Carbon is the fourth most abundant element in the Universe, with an abundance of 3×10^{-4} relative to that of hydrogen.[1] It occupies a unique position in the periodic table, owing to its ability to form stable single, double, and triple bonds. This chain-forming capability of carbon is key to its role not only as the common element in all of the molecules of life but also as the architectural backbone of the majority of observed extraterrestrial molecules. Carbon is present in around three-quarters of the molecules that have been detected in interstellar space, and all such molecules having more than five atoms contain carbon. Moreover, despite the overwhelmingly high abundance of elemental hydrogen, most of these compounds are highly unsaturated, containing a high proportion of carbon to hydrogen.

The highest concentrations and richest variety of interstellar molecules are found in dense interstellar clouds (ISCs). These clouds correspond to the laboratory equivalent of an ultrahigh vacuum, with densities of the order of 10^4 molecules cm^{-3}. They are also extremely cold by terrestrial standards, with temperatures in the range of 10−50 K. However, owing to their great size, they may contain typically the equivalent of 10−100 times the mass of our Sun. The largest confirmed interstellar molecule is cyano-polyyne $HC_{11}N$,[2] but it is highly probable that much larger carbon-containing species will be detected.

Astrophysical chemists seek to understand the chemistry that leads to the observed abundances of molecules in dense ISCs by constructing reaction networks and performing computer simulations of the molecular evolution. In recent years, the importance of reactions between electrically neutral species has

* To whom correspondence should be addressed. E-mail: d.c.clary@ucl.ac.uk.
† University College London.
‡ The University of Birmingham.
§ Université Bordeaux 1.
|| Università di Perugia.

10.1021/jp020310z CCC: $22.00
Published on Web 05/21/2002

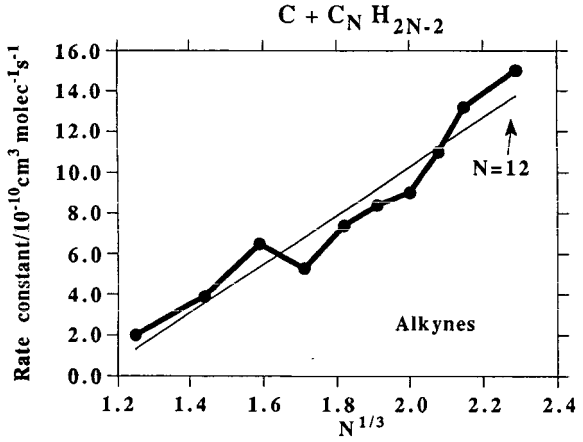

Figure 1. Experimental (circles) and theoretical (straight line) rate constants for the reaction of C(^{3}P) with alkynes C_NH_{2N-2} plotted against $N^{1/3}$.[12]

been recognized,[3−7] despite the extremely low temperatures which prevail in dense ISCs. An issue of key importance is how larger molecules are assembled and, in particular, how molecules containing chains of several carbon atoms are synthesized.

Ground-state carbon atoms, C(^{3}P), have been detected in a wide variety of astronomical environments and are also particularly abundant in dense ISCs,[8,9] where their abundance is comparable to that of CO, the second commonest molecule after H_2. Acetylene has also been observed in significant abundance.[10] The possibility of the reaction

$$C(^3P) + C_2H_2 \rightarrow \text{products} \qquad (1)$$

being important in the interstellar medium was suggested following a systematic series of kinetic experiments performed by Husain and co-workers.[11] This group found that the rate constants for C(^{3}P) reacting at room temperature with alkenes and alkynes were very large, suggesting no barriers in the potential energy surface for these reactions. A simple capture theory was applied, based on an assumed linear increase of polarizability of the reacting molecule with the number N of carbon atoms. This theory suggested that the rate constants for these reactions will depend on $N^{1/3}$, and experiment confirmed this prediction (see Figure 1).[12] Indeed, for $N > 10$, the rate constants become larger than 10^{-9} cm^3 molecule^{-1} s^{-1}, which is the same order of magnitude as those found for many ion−molecule reactions.[13] These studies thus suggested that these reactions of carbon atoms are a mechanism for the efficient production of longer carbon-chain molecules in the interstellar medium. In addition, because these reactions are very fast at room temperature, it was thought likely that they would also be fast at the typical temperatures of interstellar clouds (∼20 K).

Measurements of rate constants for the reactions of C(^{3}P) atoms with alkynes and alkenes were performed for lower temperatures down to 15 K by Sims and co-workers. They first used an indirect chemiluminescent marker technique[14] and then, very recently, employed for the first time direct vacuum ultraviolet (VUV) laser-induced fluorescence (LIF) detection of atomic carbon.[15−17] The rate constants for the reaction of C(^{3}P) with C_2H_2, C_2H_4, $CH_3CH{=}CH_2$, $CH_3C{\equiv}CH$ and $H_2C{=}C{=}CH_2$ were measured down to 15 K and found in all cases to exceed 2×10^{-10} cm^3 molecule^{-1} s^{-1} over the entire range of temperatures, in some cases exceeding 4×10^{-10} cm^3 molecule^{-1} s^{-1} at the lowest temperatures. These correspond to some of the most rapid neutral−neutral reactions yet found.

Following these theoretical and experimental studies, the rate constants of reactions of atomic carbon with various hydrocarbon species were included in the chemical reaction networks used to model interstellar clouds (ISCs).[6] These simulations confirmed that these reactions are of great importance in the synthesis of larger carbon-containing species, employing successive insertion−elimination reactions of the type[17]

$$C + C_nH_m \rightarrow C_{n+1}H_{m-1} + H$$

Among these proposed chain-building reactions, the reaction of C(^{3}P) with C_2H_2 may be seen as prototypical. It is probably one of the most important of these reactions from an astrophysical point of view,[18] and yet it is simple enough for application of first-principles electronic structure and dynamics calculations. However, despite its relative simplicity, it serves to highlight the lack of quantitative, and in many cases even qualitative, knowledge of the reaction products and their associated branching ratios. Even for this simple reaction, there exist a number of thermodynamically accessible products:

$$C(^3P) + C_2H_2(X^1\Sigma^+) \rightarrow [C_3H_2]^\dagger \rightarrow l\text{-}C_3H(X^2\Pi) + H(^2S)\ \Delta H_0{}^0 = -1.5 \text{ kJ mol}^{-1}\ ^{18,19} \qquad (2a)$$

$$\rightarrow c\text{-}C_3H(X^2B_2) + H(^2S)\ \Delta H_0{}^0 = -8.6 \text{ kJ mol}^{-1}\ ^{18,19} \qquad (2b)$$

$$\rightarrow C_3(^1\Sigma^+) + H_2\ \Delta H_0{}^0 = -104.6 \text{ kJ mol}^{-1}\ ^{20} \qquad (2c)$$

All recent ab initio calculations[19,25−27] agree that the cyclic c-C_3H isomer is more stable than the linear isomer, although only one study showed that formation of linear l-C_3H is slightly exoergic.[19] Both l-C_3H and c-C_3H have been observed by radio astronomy in a range of interstellar environments, including both cold, dense ISCs and warmer translucent clouds.[21] C_3 has also been detected both in circumstellar envelopes[22−24] and interstellar clouds.[24]

The kinetic experiments only measured the overall rate constant for reaction 1 and did not detect the products of this reaction. Kaiser and co-workers have performed an extensive series of crossed molecular beam (CMB) experiments at collision energies of 8.8, 28.0, and 45.0 kJ mol^{-1} on reaction 1, employing mass spectrometric detection of the C_3H product.[18,19] Although mass spectrometric detection precluded the ability to distinguish between l-C_3H and c-C_3H directly, from changes in the angular scattering with collision energy, they inferred that both of these isomers were formed under the conditions of their experiments, with the contribution of the latter, more exothermic channel decreasing at higher collision energies. However, the collision energies in these experiments (8.8−45.0 kJ mol^{-1}) were appreciably larger than the average energy of thermal collisions at temperatures prevailing in typical dense interstellar clouds, between 0.1 and 0.5 kJ mol^{-1}.

These molecular beam experiments were complemented by high-quality ab initio calculations of intermediates and products of the reaction.[19] The calculations suggested that both l-C_3H and c-C_3H should be formed in exothermic reactions, with c-C_3H having a slightly lower energy than l-C_3H. Several other ab initio calculations have also been performed[25−28] on this reaction and a schematic diagram of intermediate and product energetics is shown in Figure 2. Furthermore, a recent wave packet calculation was carried out on the dynamics of the reaction using a potential energy surface expressed in reduced dimensions and obtained from ab initio calculations.[28] This computation gave

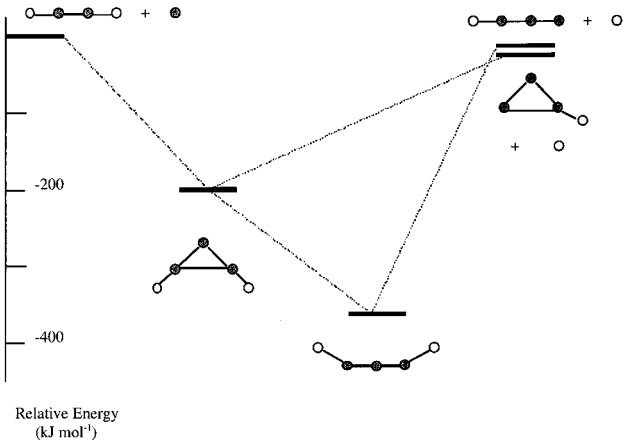

Figure 2. Schematic diagram of the intermediate and product energetics for the formation of linear and cyclic C_3H from the $C(^3P) + C_2H_2$ reaction.

cross sections and rate constants for forming both *l*-C_3H and *c*-C_3H and is discussed in more detail in this paper.

The development of an all-pulsed CMB experiment[29,30] with variable beam intersection angle and LIF detection of the H atom product allowed integral cross sections to be determined for reactions such as (2a) and (2b) down to very low relative translational energies (0.4 kJ mol^{-1} corresponding to the mean energy of a thermal distribution at 30 K).[30] The results of these experiments are discussed in detail in this article. Noticeably, the energy dependence of the integral cross sections for H production was found to be in excellent agreement with the temperature dependence of the rate constants for removal of $C(^3P)$ atoms in the reaction of $C(^3P)$ with methylacetylene and allene.[15] The agreement is less good for the reaction of $C(^3P)$ with acetylene,[30] and possible reasons for this are discussed here.

A very recent kinetic study at room temperature determined both the overall rate constant for reaction 1 (following the decay of C atoms) and the branching ratio for H-atom production (by atomic resonance fluorescence at 121.6 nm (Lyman-α)).[31] An upper limit for H production, $k_H/k_{total}=0.53 \pm 0.04$ was derived. This result, although obtained in a flow system, indicates that another channel, presumably, on energetic grounds, that leading to $C_3(X^1\Sigma_g^+) + H_2$, is contributing to the $C(^3P) + C_2H_2$ reaction (see eq 2c). (The H-abstraction pathway leading to $CH + C_2H$ is strongly endoergic ($\Delta H_0^0 \sim 120$ kJ mol^{-1}) and is open only at high collision energies;[32] therefore, it is not considered here.)

A new molecular beam study that measured angular and velocity distributions for the reaction of a beam containing $C(^3P)$ and $C(^1D)$ with C_2H_2 has also been reported,[33,34] and this also gave strong evidence for the formation of the $C_3 + H_2$ products. This work is also discussed later in this article.

For all of these reasons, the $C(^3P) + C_2H_2$ reaction has been chosen for intensive study in a complementary and collaborative series of experimental and theoretical studies that are brought together in this feature article. In section II, new rate constants measured in Birmingham for temperatures down to 15 K are described and compared with theory and other measurements. Section III presents the results of molecular beam experiments from Bordeaux on the energy dependence of the integral cross sections for the reactions of $C(^3P)$ with C_2H_2 and C_2D_2. In section IV, product angular and velocity distributions derived from molecular beam experiments performed in Perugia are reported. They provide strong evidence for the importance of the formation of $C_3 + H_2$. Calculations carried out in London are described in section V in which emphasis is placed on using first-principles electronic structure and dynamics methods to predict cross sections and rate constants for forming both linear and cyclic C_3H. Comparisons are made with some of the experimental results described in the earlier sections. In section VI, the conclusions from the various studies are made and the implications of the results for understanding the role of the $C(^3P) + C_2H_2$ reaction in the interstellar medium are discussed.

II. Low Temperature Rate Constant Measurements

II.1. Experimental Method. The rate constants for the reactions of $C(^3P)$ atoms with C_2H_2 have been measured in the Birmingham CRESU (Cinétique de Réaction en Ecoulement Supersonique Uniforme) apparatus[14−17,35] at temperatures down to 15 K. In a CRESU apparatus, low temperatures are achieved by isentropic expansion of a gas mixture, consisting predominantly (typically >99%) of a carrier gas (He, Ar, or N_2) through an axisymmetric, convergent−divergent, Laval nozzle. A supersonic flow of gas is generated in which the Mach number, the temperature, the total pressure of the gas, and the mole fractions of the components of the mixture are uniform along the flow. In all of the experiments referred to here, a small concentration of C_3O_2 was included in the flow, and $C(^3P)$ atoms were generated by pulsed laser photolysis of this precursor at 193 nm, using an excimer laser operating on ArF.[14−17] The output from this laser was directed through the gas reservoir and Laval nozzle and along the axis of the gas flow.

The kinetic decays of the $C(^3P)$ atomic concentration were monitored directly using resonant vacuum-ultraviolet laser-induced fluorescence (VUV-LIF), that is, with both excitation and observation of the fluorescence on the ($2s^22p3s\ ^3P_J - 2s^22p^2\ ^3P_J$) transition of atomic carbon. Pulses of VUV laser radiation were generated using four-wave mixing in Xe. The method is described in some detail elsewhere.[16] Briefly, dye laser radiation was tuned to 255.94 nm in order to excite Xe in a two-photon transition to its $5p^56p[2^1/_2, 2]$ state. A second pulsed dye laser could be tuned through the wavelength range between 560 and 565 nm to generate VUV radiation between 165.9 and 165.4 nm. LIF spectra of the ($2s^22p3s\ ^3P_J - 2s^22p^2\ ^3P_J$) transition in atomic carbon were recorded and confirmed that spin−orbit relaxation within the electronic ground state was achieved on a time-scale which was short relative to that for the reaction,[16] so that the rate constants that are measured correspond to those for entirely thermalized conditions.

For kinetic measurements, the VUV probe laser was set at the wavelength of the ($2s^22p3s\ ^3P_{J=1} - 2s^22p^2\ ^3P_{J=0}$) transition at 165.69 nm, and LIF signals were recorded as the time delay between the pulses from the photolysis and probe lasers was systematically varied. The recorded traces of the LIF signal versus time accurately fitted single exponential decays yielding pseudo-first-order rate constants (k_{1st}). Second-order rate constants for reaction at a particular temperature were obtained by measuring values of k_{1st}, with different concentrations of the co-reagent added to the flowing gas mixture, and plotting k_{1st} versus $[C_2H_2]$. Examples of first- and second-order kinetic plots are displayed in Figure 3.

II.2. Experimental Results for Rate Constants. Rate constants $k_1(T)$ for the reaction of $C(^3P)$ atoms with C_2H_2 at temperatures between 15 and 295 K have been reported in ref 17. They are displayed in Figure 4 as a function of temperature (T) on a log−log plot. The variation of $k_1(T)$ with T is slight, and the rate constants at all temperatures are close to the collision-determined limit. The data are fitted to the form $k(T) = A(T/298)^n$, yielding $A = (2.9 \pm 0.7) \times 10^{-10}$ cm^3 molecule^{-1} s^{-1} and $n = (-0.12 \pm 0.10)$, with statistical errors quoted as

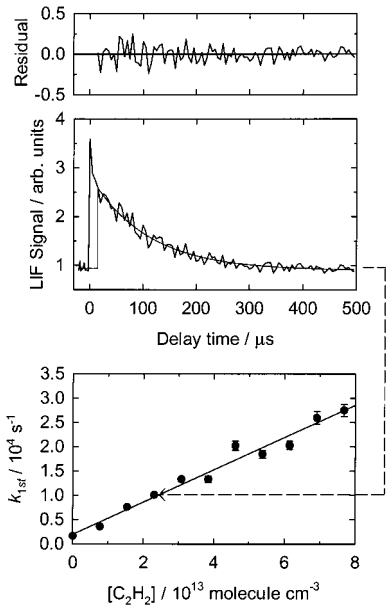

Figure 3. Typical experimental data obtained in the CRESU experiment, at a temperature of 54 K in a buffer gas of argon at a density of 5.36×10^{16} molecule cm^{-3}. The upper panels show the time-resolved decay of the C(^{3}P) VUV LIF signal in the presence of 2.31×10^{13} molecule cm^{-3} of C_2H_2. The smooth curve shows a single-exponential fit to the data, the residuals being shown in the uppermost panel. The lower panel is a plot of pseudo-first-order rate constants versus [C_2H_2], the gradient of which corresponds to the rate constant for the reaction of C(^{3}P) with C_2H_2 at 54 K.

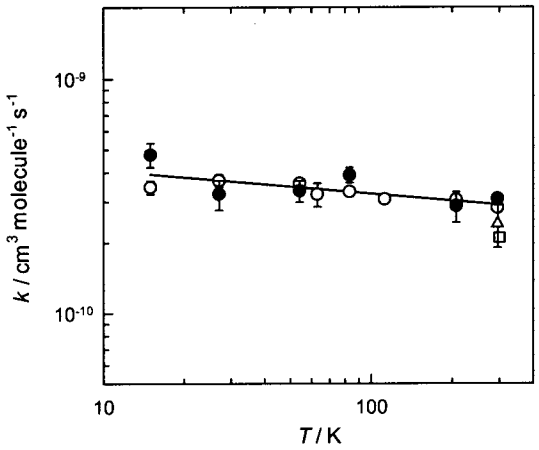

Figure 4. Rate constants for the reaction of C(^{3}P) atoms with C_2H_2 as a function of temperature plotted on a log−log scale. The filled circles (●) show the results from the present work with VUV detection, and the open circles (○) show the results of previous experiments in the CRESU apparatus using the chemiluminescent marker technique.[14] Results of other workers at room temperature are shown as an open square (□)[36] and an open triangle (△).[31] The continuous line is a fit to the CRESU data yielding: $k(T) = 2.9 \times 10^{-10}\ (T/298)^{-0.12}$ cm^3 molecule^{-1} s^{-1}.

$\pm 2\sigma$, where σ is the standard error. We have also plotted the rate constants obtained in previous studies of the reaction of C(^{3}P) atoms with C_2H_2. Except for the earlier results which we obtained using the chemiluminescent marker technique, the previous data are limited to room temperature. The present results are in good agreement with those obtained using the chemiluminescent technique. The parameters A and n found by fitting both sets of data, according each set equal weighting, are essentially identical to those given above: $A = (2.9 \pm 0.3) \times 10^{-10}$ cm^3 molecule^{-1} s^{-1} and $n = (-0.12 \pm 0.10)$. Our result at room temperature is in fair agreement with those of Haider and Husain[36] and Bergeat and Loison.[31] There is no apparent dependence of the CRESU results on the nature of the carrier gas, confirming that the experiments determine rate constants for bimolecular reactions between the unsaturated hydrocarbon and the C(^{3}P) atoms.

The kinetic measurements reported here confirm the earlier conclusion[14] that C(^{3}P) atoms react rapidly with C_2H_2 at very low temperatures. This rapidity and the fact that the rate constants are almost independent of temperature lead to two important fundamental conclusions. First, there must be no barrier on the potential energy surfaces leading from reagents to products for these reactions. This conclusion is confirmed by the new CMB experiments performed at low collision energies on the integral cross sections for reactions of C(^{3}P) atoms with C_2H_2 and C_2D_2 described in the next section. Furthermore, it appears that the rate constants of these reactions of C(^{3}P) atoms must be essentially independent of the spin−orbit state of the atom, i.e., of J. The spin−orbit states in C(^{3}P) are closely spaced with $J = 1$ only 16.4 cm^{-1} (corresponding to 23.6 K) above the lowest $J = 0$ component and $J = 2$ lying 43.4 cm^{-1} (corresponding to 62.4 K) above $J = 0$. There is a dramatic change in the relative spin−orbit populations as the temperature is reduced between 295 K (where $N_{J=0}$:$N_{J=1}$:$N_{J=2}$ = 1.0:2.77:4.05) and 15 K (where $N_{J=0}$:$N_{J=1}$:$N_{J=2}$ = 1.0:0.62:0.08). Consequently, if the rate constant for reactions of C(^{3}P) atoms depended appreciably on the J level, then we should expect to have observed a similarly strong dependence of the thermally averaged rate constants on temperature. The experimental kinetic results unfortunately provide no information about the products of the reaction of C(^{3}P) atoms with C_2H_2 at low temperatures.

Experimental data relating to the branching ratios into channels (2a), (2b), and (2c) are sparse, and no experiments which can provide such information have been carried out at temperatures or collision energies appropriate to dense ISCs.

III. Integral Cross Sections Measurements

III.1. Experimental Method. Excitation functions for the C(^{3}P) + C_2H_2 and C(^{3}P) + C_2D_2 reactions have been obtained with a crossed beam apparatus in Bordeaux. Detailed descriptions of the crossed beam machine[29] and of the laser-induced fluorescence (LIF) detection method of C(^{3}P)[15] and H($^2S_{1/2}$)[16] have already been given. Briefly, the atom beam is produced when seeding laser ablated C-atoms from a graphite rod into a pulsed, supersonic beam of a carrier gas (Ar, Ne, or He). The skimmed pulsed C(^{3}P) beam of velocity $\mathbf{v}_C$ is crossed with a skimmed pulsed supersonic acetylene beam of velocity $\mathbf{v}_{C_2H_2}$ at an intersection angle θ. The relative translational energy, E_c, of reagents of reduced mass μ is tuned by varying the beam intersection angle between $\theta = 22.5°$ and 90° without needing to change the beam source conditions and hence the laboratory beam velocities:

$$E_c = 1/2\,\mu(\mathbf{v}_C^{\,2} + \mathbf{v}_{C_2H_2}^{\,2} - 2\mathbf{v}_C\,\mathbf{v}_{C_2H_2}^{\,2}\cos\theta)$$

and more extended ranges of energies are covered by combining different sets of laboratory beam velocities. The H or D($^2S_{1/2}$) reaction product is probed in the beam crossing region by one-photon resonant LIF using the ($^2S_{1/2} \leftrightarrow {}^2P°_J$) Lyman-α transition at 121.567 nm for H (121.534 nm for D) with a pulsed tuneable laser beam propagating perpendicular to the scattering plane.

III.2. Results for Cross Sections. First attempts to obtain a reactive signal with C(^{3}P) + C_2H_2 were not successful, because of an intense background signal in the spectroscopic detection

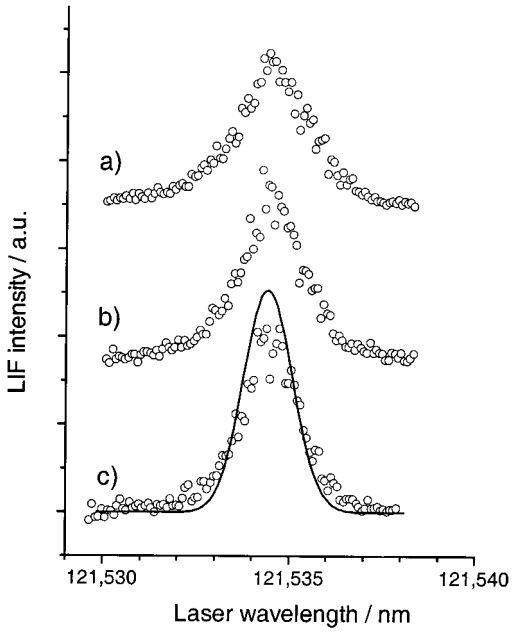

Figure 5. LIF spectra of D atoms at Lyman-α. Open circles: D atoms from $C(^3P) + C_2D_2$ reactive collisions at $E_c = 25.5$ (a), 8.5 (b), 0.39 kJ mol^{-1} (c); solid line: apparatus function determined from cold H atoms in the C-beam and shifted to the D-line position. Spectra are normalized to unit area. Adapted from ref 30.

of H at Lyman-α (121.567 nm), which arose from H atoms generated in the ablation process and cooled by the supersonic expansion of the carrier gas. By contrast, $C(^3P) + C_2D_2$ experiments were background free and exhibited very high signal-to-noise ratio. Doppler profiles of the D atom product could be recorded by scanning the laser wavelength around the center of the Lyman-α transition (121.534 nm) at selected translational energies.[30] Three of them are displayed in Figure 5 along with the apparatus function (i.e., the line width of the Lyman-α laser beam). At the lowest translational energy of 0.39 kJ mol^{-1}, the Doppler profile is almost identical to the apparatus function. This emphasizes that the out-of-plane velocity vectors of the recoiling D atoms are distributed narrowly around the relative velocity, which shows that the total available energy and hence the reaction exoergicity is very low. Note that the broadening of the Doppler profile with increasing relative translational energy remains moderate, even at the highest energy accessed, $E_c = 23.2$ kJ mol^{-1}. Note also that these narrow Doppler profiles cannot originate from reaction of $C(^1D)$ present as an impurity in the $C(^3P)$ beam, because the high translational energy release given by $C(^1D) + C_2D_2$ would give rise to a very broad Doppler profile.

Cross section measurements were performed with the laser tuned at the maximum of absorption and scanning the beam intersection angle for different sets of reagent laboratory velocities. Relative values of the cross sections were obtained by dividing the averaged signal intensities by the relative velocities of the reagents. The normalized excitation function (in arbitrary units) displayed in Figure 6 is well represented by $\sigma \propto \{E_c\}^{\alpha}$ functionality with $\alpha = -0.71 \pm 0.01$.[30] The integral cross-section is monotonically increasing with decreasing kinetic energy, with no sign of a downward curvature in the low energy part that could have suggested the existence of a threshold below the energy range scanned. The $C + C_2D_2$ reaction has clearly no barrier at all.

$C(^3P) + C_2H_2$ cross section measurements could be carried out between 0.38 and 25.5 kJ mol^{-1} relative translational energy after strong reduction of the background arising from cold H

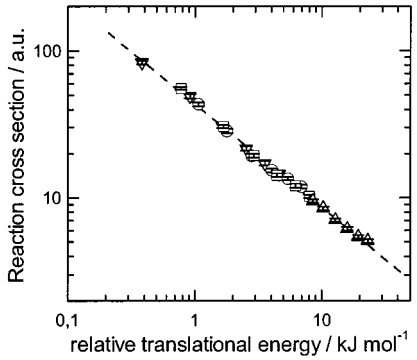

Figure 6. Normalized excitation function of the $C + C_2D_2$ reaction. Experimental conditions: $\mathbf{v}_C = 810$ m s^{-1} and $\mathbf{v}_{C_2D_2} = 700$ m s^{-1}: down triangles (▽); $\mathbf{v}_C = 1080$ m s^{-1} and $\mathbf{v}_{C_2D_2} = 700$ m s^{-1}: circles (○); $\mathbf{v}_C = 1080$ m s^{-1} and $\mathbf{v}_{C_2D_2} = 870$ m s^{-1} beam: squares (□); $\mathbf{v}_C = 2180$ m s^{-1} and $\mathbf{v}_{C_2D_2} = 870$ m s^{-1}: up triangles (△); dashed line: fit with $\alpha = -0.71$ (see text). Adapted from ref 30.

atoms in the C beam. These experiments finally establish without any ambiguity that the H-atom elimination channel has no potential barrier. An excitation function similar to the one displayed in Figure 6 was obtained with a slightly more pronounced slope, characterized by $\alpha = -0.80 \pm 0.03$.

These cross section measurements have important implications for the reaction energetics. A somewhat controversial point is the energies of the reaction product asymptotes with respect to that of $C(^3P) + C_2H_2(X^1\Sigma^+)$.[37] This is of astrophysical significance because a reaction channel can be inhibited by any slight endoergicity in the physical conditions of cold ISCs. Ab initio calculations predict c-C_3H (X^2B_2) + $H(^2S_{1/2})$ to be below l-$C_3H(X^2\Pi_{1/2}) + H(^2S_{1/2})$[19,25-27] in energy, but only one study claims both pathways to be slightly exoergic.[19] Analogous calculations performed with the same basis set as the latter study on the isotopic variant $C + C_2DH \rightarrow C_3D + H$ reaction give[38]

$$C(^3P) + C_2HD(X^1\Sigma^+) \rightarrow c\text{-}C_3D(X^2B_2) + H(^2S_{1/2}) \qquad \Delta H_0^0 = -9.2 \text{ kJ mol}^{-1} \quad (3a)$$

$$C(^3P) + C_2HD(X^1\Sigma_g^+) \rightarrow l\text{-}C_3D(X^2\Pi_{1/2}) + H(^2S_{1/2}) \qquad \Delta H_0^0 = -0.3 \text{ kJ mol}^{-1} \quad (3b)$$

The reaction energies for $C(^3P) + C_2D_2$ can be estimated when introducing the difference in dissociation energies between DCC−H ($D_0 = 552.0 \pm 0.6$ kJ mol^{-1}) and DCC-D ($D_0 = 559.3 \pm 0.6$ kJ mol^{-1})[39]:

$$C(^3P) + C_2D_2(X^1\Sigma_g^+) \rightarrow c\text{-}C_3D(X^2B_2) + D(^2S_{1/2}) \qquad \Delta H_0^0 = -1.9 \text{ kJ mol}^{-1} \quad (4a)$$

$$C(^3P) + C_2D_2(X^1\Sigma_g^+) \rightarrow l\text{-}C_3D(X^2\Pi_{1/2}) + D(^2S_{1/2}) \qquad \Delta H_0^0 = +7.0 \text{ kJ mol}^{-1} \quad (4b)$$

where we emphasize that there are likely to be quite large uncertainties in these ΔH_0^0 values. The excitation functions of $C(^3P) + C_2H_2$ and $C(^3P) + C_2D_2$ establish clearly that at least one channel is without any barrier and hence exoergic in each case. Comparison of the width of the D atom Doppler profile of $C(^3P) + C_2D_2$ at $E_c = 0.39$ kJ mol^{-1} with the width of the apparatus function in Figure 5c shows very little difference which also means that the reaction exoergicity is very low, consistent with the mean value $\Delta H_0^0 = -1.9$ kJ mol^{-1} calculated for reaction 4a.

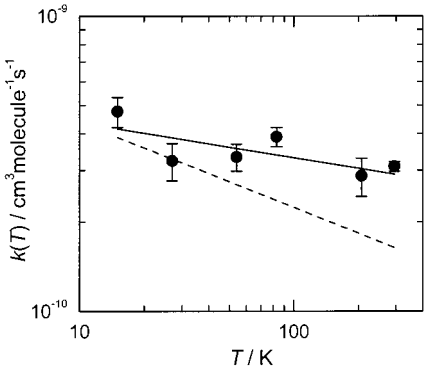

Figure 7. Rate constants for the reaction of C(^{3}P) atoms with C_2H_2 as a function of temperature plotted on a log−log scale. The filled circles (●) show the results from the present work with VUV detection. The solid line shows the fit to CRESU data. The dashed line shows the rate constant estimates derived from integral cross sections, and normalized to CRESU result at 295 K, assuming a branching ratio, $\rho = (k_{2a}+k_{2b})/(k_{2a}+k_{2b}+k_{2c}) = 0.53$.

Temperature dependent thermal rate constants $k(T)$ and kinetic energy dependent reaction cross sections $\sigma_{reac}(E_c)$ can be compared through the following relationship, assuming that the reaction cross-section, σ_{reac}, is independent of the internal states of the reagents:

$$k_{calc} = \left(\frac{8k_BT}{\pi\mu}\right)^{1/2} \int_0^\infty \sigma_{reac}(E_c)(E_c/k_BT)\, d(E_c/k_BT)$$

If it is assumed that the functional form $\sigma_{measured} \propto \{E_c\}^\alpha$ (in arbitrary units), determined in the crossed beam experiments, is representative of the total reaction cross section, then integration leads to $k(T) \propto T^n$, with $n = \alpha + 1/2$. This yields $n = -0.30 \pm 0.03$, which compares reasonably, but not perfectly, with the value obtained in the CRESU experiments (-0.12 ± 0.10) discussed in the previous section (see Figure 7).

A possible explanation of the deviation observed could be that the C(^3P_J) reactivity depends on the spin−orbit state, J. The two experiments are indeed conducted with different relative J-populations: they are almost constant in the crossed beam experiments across the entire 0.38−25.5 kJ mol^{-1} energy range, whereas they strongly vary in the kinetic measurements between 295 and 15 K.[17] However, perfect agreement with the CRESU results was found in the case of the reactions of C(^{3}P) with methylacetylene and allene.[15] Furthermore, a significant spin−orbit effect on reactivity would result in a significant departure from the simple $k(T) \propto T^n$ functionality experimentally observed, which also justifies a posteriori the assumption made.

Another factor that could account for the observed deviation is the occurrence of the H_2-elimination channel reaction 2c. If the branching ratio for H production, $\rho = (k_{2a} + k_{2b})/(k_{2a} + k_{2b} + k_{2c})$, is temperature dependent, it will result in a deviation between CRESU results, which give the overall reaction rate constant, k_{CRESU}, and the present results, which yield an estimate of the rate constant for the H-elimination channel, k_{calc}. In fact, the ratio k_{calc}/k_{CRESU} increases from 0.53 to 0.8 when the temperature decreases from 295 to 15 K (note that the calculated rate constant is normalized to $k_{calc}(295\ K) = \rho(295\ K) \times k_{CRESU}(295\ K)$ with $\rho(295\ K) = 0.53$).[31] This trend is thus consistent with the above stated hypothesis (see Figure 7).

IV. Differential Cross Sections Measurements

IV.1. Experimental Method. In Perugia, a molecular beam investigation has been undertaken on the dynamics of C atom reactions with unsaturated hydrocarbons using continuous supersonic beams containing both ground-state C(^{3}P) and first excited-state C(^{1}D). A special feature is that both angular and velocity distributions have been measured. Reactions studied include those with acetylene, methylacetylene, and ethylene.[34] By studying reactions of C(^{3}P) and C(^{1}D) under the same experimental conditions, the reaction dynamics of both C(^{3}P) and C(^{1}D) have been derived, and this has allowed the effect of electronic excitation on the reaction dynamics to be explored. Here we focus on the reaction of C atoms with acetylene.

The C(^{3}P,^{1}D) + C_2H_2 reactions occur over the triplet/singlet C_3H_2 potential energy surfaces (PESs; see Figure 8) which contain several isomers: propynylidene (i.e., propargylene, HCCCH) is the simplest acetylenic carbene, propadienylidene is the simplest vinylidene carbene (H_2CCC), and cyclopropenylidene (c-C_3H_2) is the smallest cyclic alkyne. These highly reactive molecules are fundamentally important not only within the context of organic chemistry but also within the context of the chemistry of the interstellar medium and hydrocarbon combustion. Interestingly, not only C_3H but also C_3 has been observed in space[21−24,40,41] (C_3 also in comets)[21,42] and may well be produced by the above reactions. The PESs depicted in Figure 8 will serve as the basis for discussion of the differential cross section results (see below).

The experiments were performed using a crossed molecular beam apparatus which has been described in detail else-

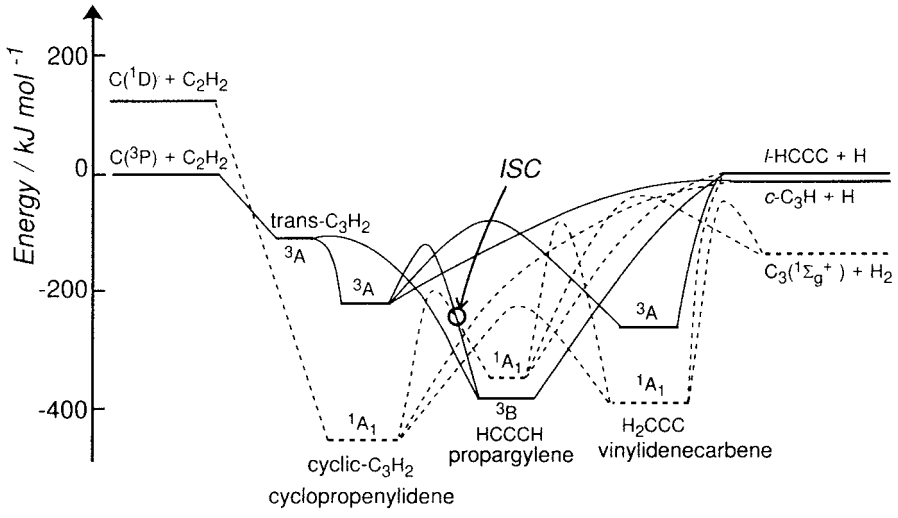

Figure 8. Schematic representation of the singlet and triplet C_3H_2 potential energy surfaces adapted from refs 19, 20, 25−27, and 43.

where.[33,44] The collison energy was 29.3 kJ mol^{-1}. Briefly, two continuous, supersonic beams of the reactants, well collimated in angle and velocity, are crossed at 90° under single collision conditions in a large scattering chamber kept below 5×10^{-7} mbar. The angular and velocity distributions of the reaction products are recorded by a triply differentially pumped, ultra-high-vacuum (10^{-11} mbar) electron impact ionizer followed by a quadrupole mass filter. The whole detector unit can be rotated in the plane of the two beams around their intersection axis. The velocity of reactants and products is derived by using time-of-flight (TOF) analysis.

In the present work, intense continuous supersonic beams of C atoms are produced by means of a rf discharge in a water-cooled quartz nozzle ($\phi = 0.3$ mm)[33,44] which operates at high rf power (300 W) and relatively high pressure (~300 mbar) on dilute (few percent) mixtures of a suitable precursor molecule, CO_2, in He. The C beam had an angular divergence of 2.3°, a peak velocity of 2585 m s^{-1}, and speed ratio of 7.4. Atomic carbon is produced mainly in the ground ^{3}P state, with also a significant concentration in the excited ^{1}D state (lying 1.26 eV above the ground state).[45] The C beams contain only 2−3% C_2 and no detectable C_3. The acetylene beam was produced by expanding neat gas through a resistively heated stainless steel nozzle ($\phi = 0.1$ mm) using on-line traps to remove acetone impurities; the peak velocity and speed ratio were of 834 m s^{-1} and 6.4, respectively, and the angular divergence was about 5°.

Product angular distributions were recorded by modulating the acetylene beam at 160 Hz for background subtraction and taking at least 4−5 scans at each mass (typical counting times were 50 s at each angle). Product TOF distributions were recorded at selected angles using the pseudorandom TOF technique at 5 μs/channel (typical counting times varied from 30 to 90 min depending on signal intensity).

For the physical interpretation of the experimental distributions, it is necessary to transform the laboratory (LAB) distributions into the center-of-mass (CM) system,[33] where the CM product flux can be factorized into a product angular $T(\theta)$, and translational energy, $P(E'_T)$ distributions. The CM functions are actually derived by a forward convolution fit of the laboratory distributions, which are calculated taking into account the transformation Jacobian and the averaging over the experimental parameters. The procedure is repeated until a satisfactory fit of the LAB distributions is achieved and the CM functions so determined are the best-fit functions.

IV.2. Results of Differential Cross Sections. The reactions C(^{3}P,^{1}D) + C_2H_2($X^1\Sigma^+$) with a collision energy of 29.3 kJ mol^{-1} were investigated by measuring product angular and TOF distributions at all possible product masses, that is $m/e = 37$ (C_3H^+) and 36 (C_3^+). Figure 9 depicts the m/e=37 and 36 angular distributions, whereas Figure 10 shows a TOF distribution for $m/e = 37$ and 36 at $\Theta = 25°$. As can be seen, the $m/e = 36$ angular distribution is different from that at $m/e = 37$, being significantly wider, and also the TOF spectrum at $m/e = 36$ is different from that at m/e=37, being somewhat faster. This indicates that the $m/e = 36$ signal does not come completely from dissociative ionization of the C_3H product in the ionizer, as was concluded in an earlier study,[19] but it also arises from a distinct, dynamically different reaction channel. Clearly, the $m/e = 37$ product corresponds to the H-displacement channel leading to C_3H + H products, and the angular distribution and TOF data indicate that the C_3H product originates from both the C(^{3}P) and the C(^{1}D) reactions. From the best-fit of the $m/e = 37$ angular and TOF distributions, the CM product angular and

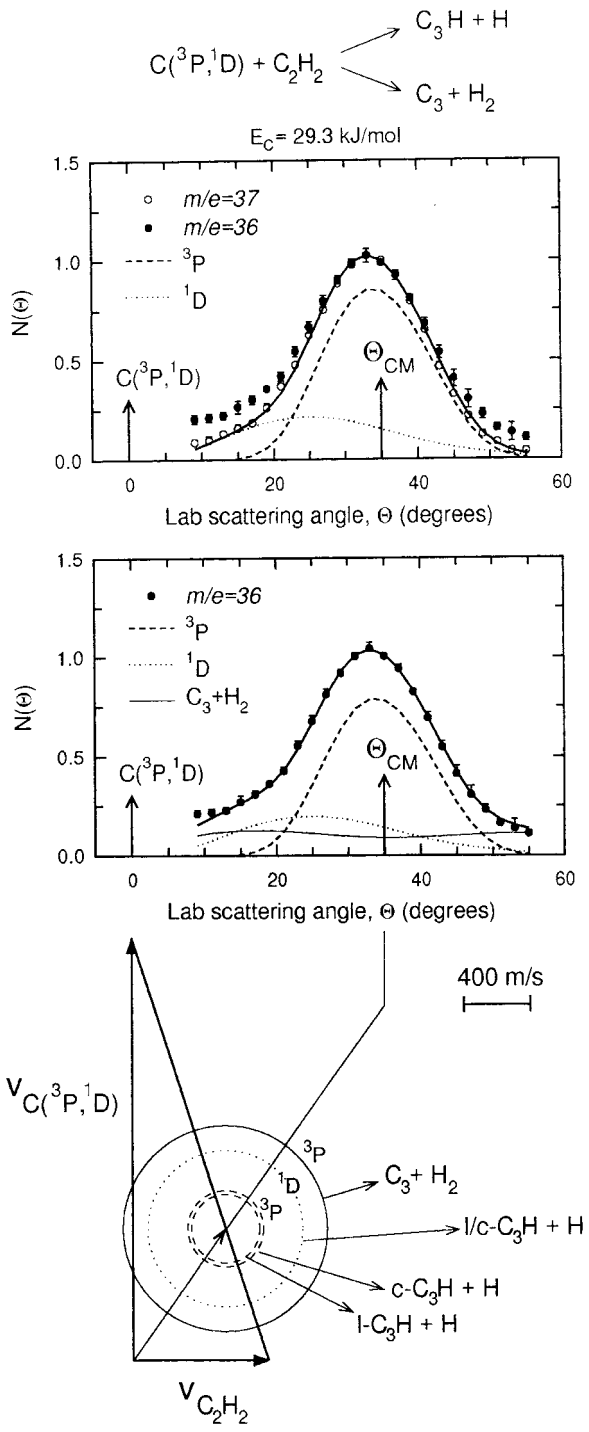

Figure 9. (Top) Lab angular distributions of products at $m/e = 36$ (solid circles) and 37 (open circles) from the reaction C(^{3}P,^{1}D) + C_2H_2 at $E_c = 29.3$ kJ mol^{-1}. Dashed and dotted lines are the calculated contributions from the ^{3}P and ^{1}D reaction, respectively, to the H elimination channel; the continuous line is the total best-fit to the $m/e = 37$ data (H channel from C(^{3}P,^{1}D)). (Bottom) Lab angular distribution of product at $m/e = 36$ (solid circles) from the reaction C(^{3}P,^{1}D) + C_2H_2 at $E_c = 29.3$ kJ mol^{-1}. Dashed and dotted lines are the calculated contributions from the ^{3}P and ^{1}D reaction, respectively, to the H elimination channel, whereas the light, continuous line is the contribution from the H_2 elimination channel from C(^{3}P) reaction; the heavy continuous line is the total best fit to the $m/e = 36$ data (H channel from C(^{3}P,^{1}D) and H_2 channel from C(^{3}P)). The corresponding Newton diagram of the experiment is also shown with the various circles representing the maximum velocity that the C_3H and C_3 products from the indicated ^{3}P and ^{1}D reactions can attain, assuming that all of the available energy is channelled into translation.

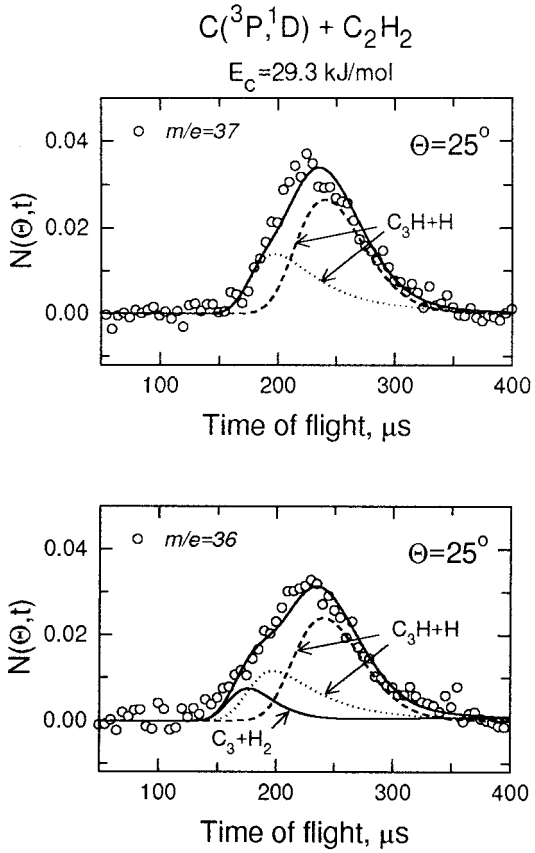

Figure 10. $m/e = 37$ (top) and 36 (bottom) product time-of-flight distributions at $\Theta = 25°$ from the $C(^3P,^1D) + C_2H_2$ reaction at $E_c = 29.3$ kJ mol^{-1} (line symbols are as for angular distributions at $m/e = 37$ and 36 in Figure 9).

translational energy distributions for the H-displacement channel from $C(^3P)$ and $C(^1D)$ were derived.[34]

The $P(E'_T)$ distribution for the $C(^3P)$ reaction is depicted with a dashed line in Figure 11b; as can be seen, the distribution extends to the maximum total available energy and it is not possible to distinguish whether the linear or cyclic C_3H isomer is formed because of the very small energy difference between the two isomers (assuming the ab initio energetics of ref 19). About 43% of the total available energy is channeled into product translation, which indicates that the C_3H radical is formed with a significant degree of internal excitation. The C_3H CM angular distribution (see dashed line in Figure 11a) is nearly backward−forward symmetric with some more intensity in the forward direction, indicating that the reaction is proceeding through an "osculating complex", i.e., a complex whose lifetime is comparable to its rotational period. It is interesting to note that the angular distribution of the ^1D reaction leading to $C_3H + H$ (not shown)[34] exhibits a forward-to-backward scattering ratio much larger than that of the ^3P reaction, consistent with an expected singlet complex lifetime much shorter than the triplet complex lifetime because of the much larger exoergicity of the ^1D reaction.

The wider LAB angular distribution and the faster TOF distributions at $m/e = 36$ indicate that a more exoergic reaction pathway also contributes to the overall reaction. This must be the H_2 elimination channel leading to $C_3(X^1\Sigma_g^+) + H_2(X^1\Sigma_g^+)$ formation, which is the only other energetically allowed pathway (see Figure 8). Hence, three distinct reactive channels contribute to the $m/e = 36$ signal in Figure 9: the $C_3H + H$ channel coming from both the triplet and singlet reactions, with the C_3H product partly cracking in the ionizer, and the $C_3 + H_2$ channel.

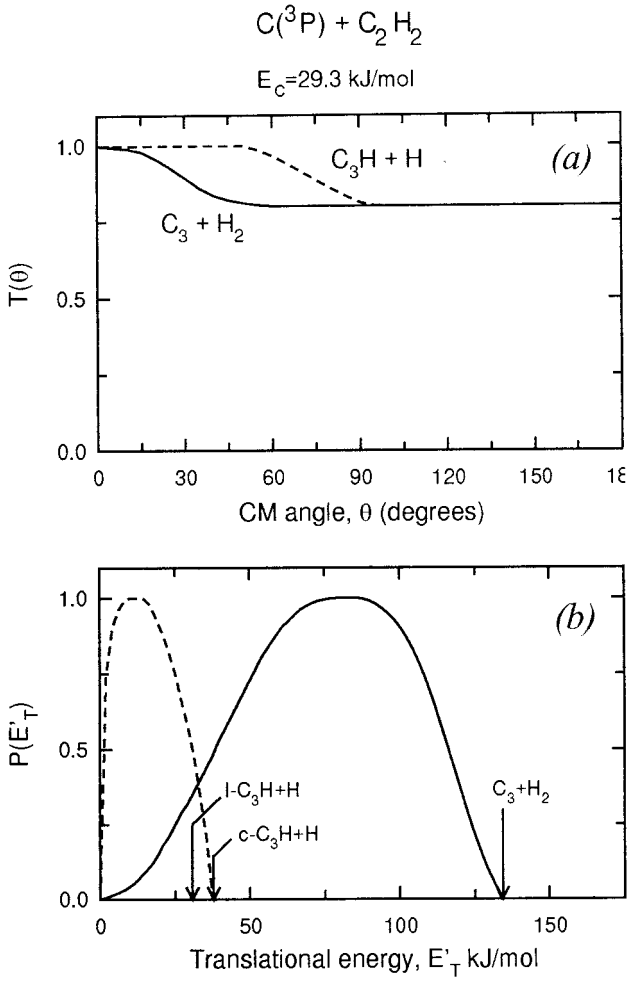

Figure 11. Best-fit CM product angular (a) and translational energy (b) distributions for the C_3H (dashed line) and C_3 (continuous line) forming channels from the reaction $C(^3P) + C_2H_2$ at $E_c = 29.3$ kJ mol^{-1}. The total available energy for the $C_3H + H$ and $C_3 + H_2$ channels is indicated with an arrow.

The C_3 CM angular distribution is nearly backward−forward symmetric (see the solid line in Figure 11a) with only a slight preference for forward scattering, indicating the intermediacy of a long-lived complex which just starts to osculate. The corresponding $P(E'_T)$ is shown in Figure 11b (solid line): interestingly, the extent of the distribution is consistent with the energetics of the $C(^3P) + C_2H_2 \rightarrow C_3(X^1\Sigma_g^+) + H_2$ reaction. Assuming that the transmission through the quadrupole mass filter of the $m/e = 36$ and 37 ions are the same and that the ionization cross sections and fragmentation patterns to C_2 and C containing fragments of C_3H and C_3 are also the same, a ratio of cross sections $\sigma(C_3+H_2)/[\sigma(C_3+H_2)+\sigma(C_3H+H)]$ of 0.37 is derived.

The only way to rationalize the formation of $C_3(X^1\Sigma_g^+) + H_2(X^1\Sigma_g^+)$ from the $C(^3P) + C_2H_2$ reaction, a spin-forbidden pathway, is to invoke the occurrence of intersystem crossing from the triplet to the singlet PES. Indeed, a recent, detailed theoretical study[27] on the C_3H_2 singlet and triplet PESs found evidence for this between triplet propargylene and singlet cyclopropylidene, which offers a solid rationale of the present experimental results.

Interestingly, these findings are also corroborated by the very recent kinetic work at room temperature of Bergeat and Loison.[31] The kinetic value of 0.53 ± 0.04 for the branching ratio $k(C_3H + H)/[k(C_3 + H_2) + k(C_3H + H)]$ compares well

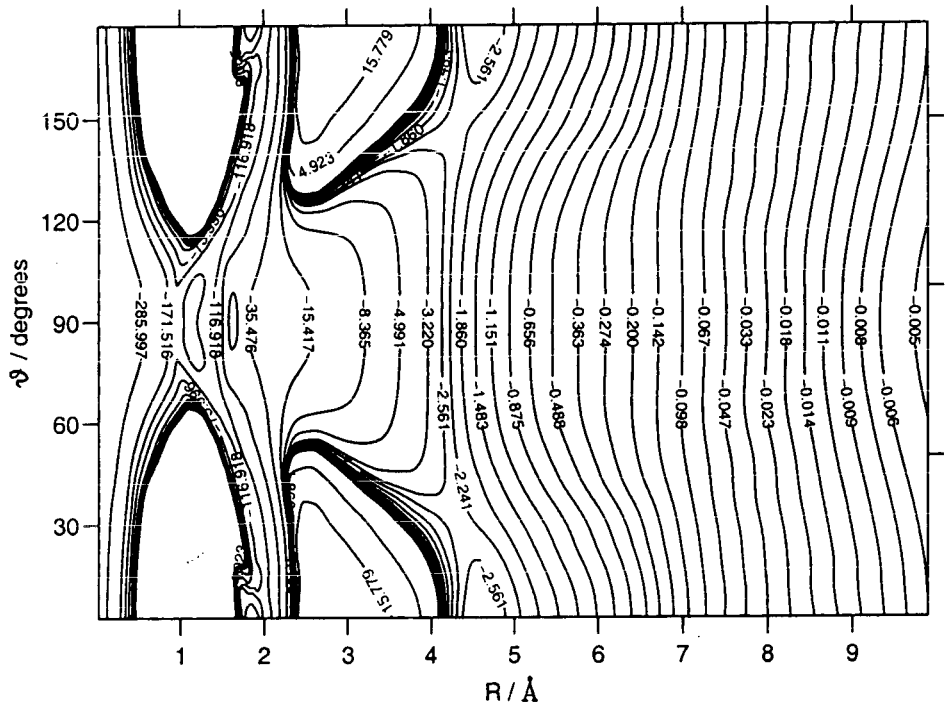

Figure 12. Reduced dimensionality potential energy surface for the $C(^3P) + C_2H_2$ reaction in terms of the coordinates R and θ.[28] The contours are in kJ mol^{-1}. The angle of the collision, $\theta = 90°$, corresponds to the perpendicular insertion of $C(^3P)$ between the two C atoms of C_2H_2, whereas 0° and 180° both correspond to insertion between the C and H atoms.

with the value of 0.63 obtained here within the uncertainty (about ±0.10) of our determination. However, the kinetic branching ratio corresponds to an average collision energy of about 4 kJ mol^{-1}, significantly lower than that of the present molecular beam study. Because the branching ratio between H and H_2 elimination is expected to be energy dependent, kinetic measurements at different temperatures and crossed beam experiments at different collision energies are desirable. Finally, intersystem crossing was also invoked to rationalize the formation of $C(^3P) + C_2H_2$ in the photodissociation of singlet C_3H_2.[46]

In the previous crossed beam study of this reaction by Kaiser et al.,[18,19] at comparable collision energies, the $m/e = 36$ and 37 angular and TOF distributions were found to be identical and this suggested that the $C(^3P) + C_2H_2$ reaction forms only $C_3H + H$. However, these pulsed experiments were characterized by some uncertainty because of the relatively low signal-to-noise ratio (S/N) in the determination of the laboratory angular distributions from measured TOF spectra and because of the presence of C_2 and C_3 clusters in the pulsed C beams; in fact, C_2 and C_3 are known to react with unsaturated hydrocarbons, and elastically scattered C_3 at $m/e = 36$ may have been an interference in the identification of all primary reaction products. In contrast, the observation of the $C_3 + H_2$ channel in our study was easily possible because of the absence of C_3 in the C beam and of the high S/N of the experiment (see Figure 9).

The molecular beam results from Perugia suggest the following mechanism for H and H_2 formation in the $C(^3P) + C_2H_2$ reaction: $C(^3P)$ adds to the acetylenic π-bond leading to *trans*-HCCHC/*cyclic*-C_3H_2 which isomerize to the more stable triplet propargylene; the latter can undergo CH bond cleavage to *l*-C_3H + H (but *c*-C_3H can also be formed from *c*-C_3H_2 by CH bond rupture before isomerization) or inter system crossing to singlet cyclopropenylidene, which in turn can isomerize to singlet propargylene and/or singlet vinylidene and lead, by (1,3) H_2 and/or (1,1)H_2 elimination, respectively, to $C_3(X^1\Sigma_g^+) + H_2$ formation. The large exit potential barrier (~100 kJ mol^{-1}) for H_2 elimination found in the ab initio calculations[27] is fully consistent with the large fraction (56%) of energy that is found experimentally to be released into product translation.

The direct, unambiguous observation that the molecular products, $C_3(X^1\Sigma_g^+) + H_2$, can be formed from the $C(^3P) + C_2H_2$ reaction indicates that intersystem crossing is facile in the C_3H_2 system. It is expected to be highly favored by the long-lived nature[26] of the strongly bound triplet propargylene intermediate which is deeply embedded in the singlet PES manifold (see Figure 8). The observation that the $C_3 + H_2$ channel is comparable in importance to the $C_3H + H$ channel at the experimental collision energy (the branching ratio is expected to be collision energy dependent) may have important consequences in establishing the role of this reaction in the modeling of interstellar chemistry networks. $C_3(X^1\Sigma_g^+)$ may also be able to undergo subsequent reactions with other unsaturated hydrocarbon molecules that, although known to be characterized by significant activation barriers,[47] may occur readily at the high temperatures (up to 4000 K) of outflows of carbon stars, leading to the formation of hydrogen deficient hydrocarbon molecules/radicals.

V. Calculations

V.1. Theoretical Method. A combined electronic structure and dynamics calculation was carried out on the $C(^3P) + C_2H_2$ reaction.[28] A reduced dimensionality method was used in which a potential energy surface was constructed in two degrees of freedom, R and θ, where R is the length of the vector R from the $C(^3P)$ atom to the center of mass of C_2H_2 and θ is the angle R makes with the C_2H_2 bond axis. The electronic structure calculations were done at the CCSD(T) level with a cc-pVDZ basis set.[48] With R and θ held on a grid of fixed positions, the other degrees of freedom were optimized. The effective potential obtained in this way for the entrance channel of the reaction is shown in Figure 12. There are no barriers above the reactant energy to the formation of both cyclic and linear C_3H. Linear

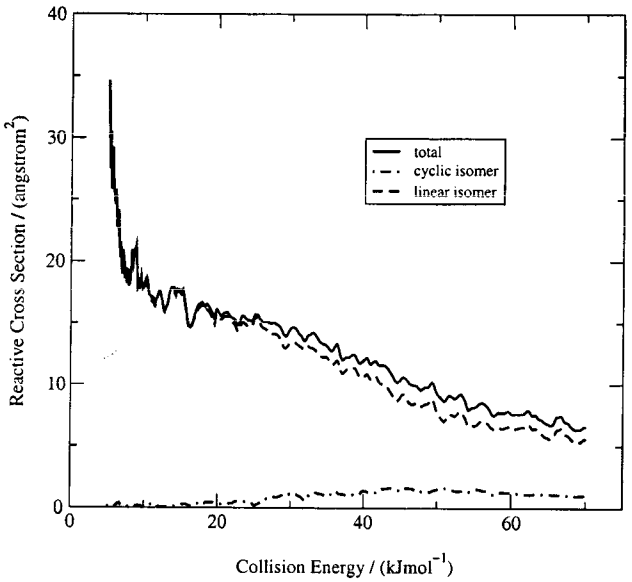

Figure 13. Wave packet calculation of cross sections for forming linear and cyclic isomers of C_3H.

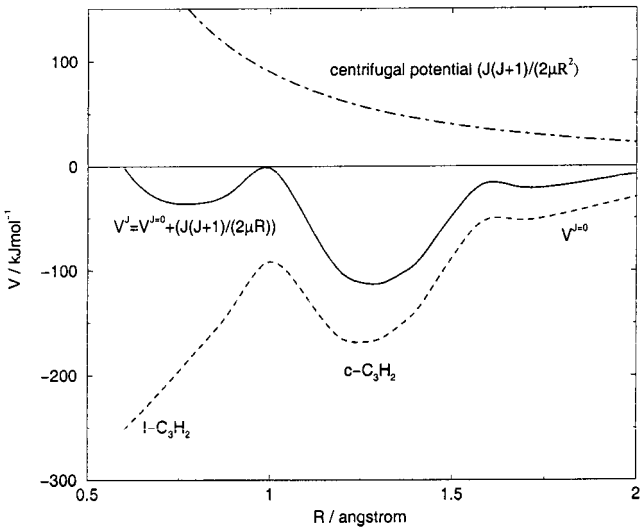

Figure 14. Effective potential (with $\theta = 90°$) for forming *c*-C_3H and then *l*-C_3H (dotted line) for $J = 0$. The effective potential for $J = 50$ is shown as an unbroken line and the pure centrifugal potential as a dashed−dot line.

C_3H can be formed either by insertion between the two C atoms or between the C and H atoms. Only one electronic potential surface was considered, and curve-crossing was neglected.

This effective potential surface was used in calculations[28] carried out using the wave packet method[49] with two degrees of freedom (R,θ). The method involved performing the wave packet calculations in the entrance channel to the reaction, without coordinate transformations and then calculating the probability for forming the C_3H_2 intermediate with C_3 in either linear or cyclic geometries. Repetition of the calculations for different values of the total angular momentum J using the coupled-states approximation gave cross sections for forming these linear or cyclic intermediates which were identified with the linear or cyclic C_3H products. Because the dissociation of H from C_3H_2 is a barrier-less process,[19] this is thought to be a valid approximation. The wave packet calculations were done using the Lanczos propagation method[49] with a discrete variable representation for R and θ.[50] After passing the dividing lines defining the linear or cyclic intermediates, the wave packet is absorbed by a negative imaginary potential to prevent reflection from the grid boundary.[51]

Calculations of total reaction cross sections and rate constants were also done with the same potential surface by using the adiabatic capture centrifugal sudden approximation (ACCSA).[52] This method does not give branching ratios but does have the advantage of being most valid in the limit of very low energies when the wave packet calculations are difficult to converge. However, back reflection of flux and inelastic effects are not treated in this technique, which is a disadvantage compared to the wave packet approach. Thus the ACCSA is expected to give an upper bound to the reaction cross section. In the past, the ACCSA has often been applied just with the longer-range terms of the intermolecular potential,[52] but the method can be used with a more complete potential, which is the case here.

V.2. Results of Calculations. Figure 13 shows the wave packet calculations of cross sections for forming the linear and cyclic isomers of C_3H. It is seen that the cross section for forming the linear isomer is by far the largest at lower energies and only at higher energies does the cross section for forming the cyclic isomer become significant.

The reason for this effect can be associated with the effective potentials for forming the linear or cyclic isomers (Figure 14). It can be seen that, for $J = 0$, there is a minimum in the effective potential for forming the cyclic isomer, but the barrier between the cyclic and linear isomers is below the C(^{3}P) + C_2H_2 asymptotic energy. Therefore, when $J = 0$, there is nothing to prevent the linear isomer from being formed. Higher J values give a centrifugal energy that raises the cyclic−linear barrier above the asymptote, and thus, the cyclic isomer becomes preferred for larger J values which become important only for higher collision energies. It should be noted that a qualitative analysis of the molecular beam results suggested a preference for production of the cyclic isomer at lower energies.[19]

Another result from the wave packet calculations is that the cross section for C(^{3}P) inserting between the two C atoms of C_2H_2 is nearly the same as that for insertion in the C−H bonds. In principle, this prediction could be tested by reacting C_2H_2 with ^{13}C.

The wave packet calculations are not valid at very low collision energies, but they do have the advantage that rotationally inelastic effects and back-reflection of reactive flux are treated explicitly, unlike the capture cross sections.[52] The cross sections for use in calculating rate constants were thus calculated by noting that the ratio of total cross sections calculated by the wave packets to those calculated by the ACCSA was close to a constant over the collision energy range considered and this constant was used to scale the ACCSA rate constants.[28] Figure 15 shows the calculated rate constants and compares with the latest experimental results described in section II. It can be seen that the scaled-ACCSA rate constants agree well with experiment, except at very low temperatures. It should be noted that the leading term of the potential depends on R^{-6} which gives a $T^{1/6}$ dependence of the rate constants at very low temperatures.[12] At higher temperatures, the overall rate constant is predicted to decrease as the temperature increases. This is because the rate constants, selected in the initial rotational states j of C_2H_2, decrease with an increase in j, and larger j values have a more significant Boltzmann weighting at higher temperatures.[52] These two opposite effects combine to produce a predicted maximum in the rate constant as a function of temperature. This maximum has not yet been observed and might require measurements at temperatures lower than 15 K.

Figure 16 compares the energy dependence of the computed total integral reaction cross sections with the experimental

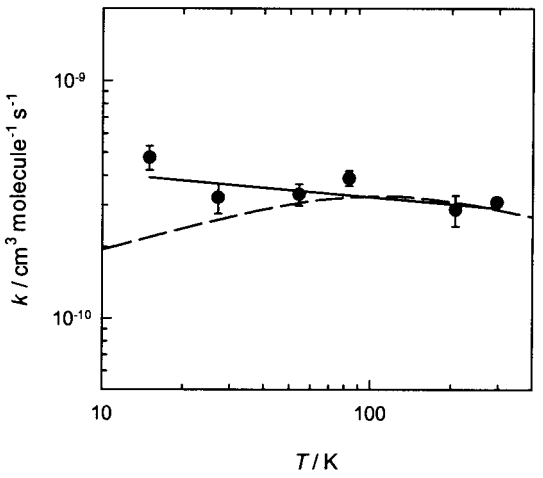

Figure 15. Rate constants for the reaction of C(^{3}P) atoms with C_2H_2 as a function of temperature plotted on a log−log scale. The filled circles (●) show the results from the present experimental work with VUV detection. The dashed line shows the theoretical results extracted from the wave packet calculations as described in the text.

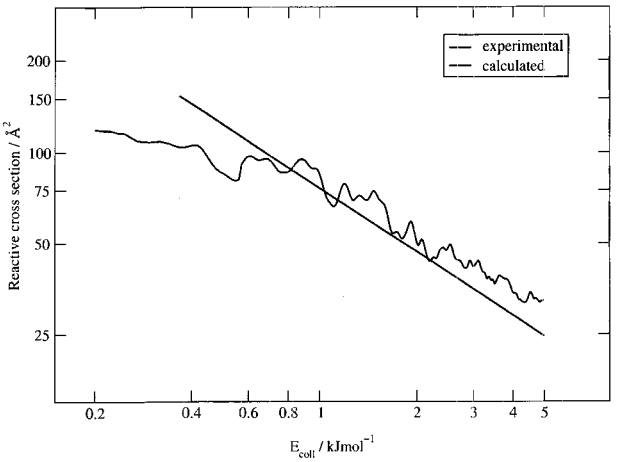

Figure 16. Plot of logarithm of the integral cross sections for the C(^{3}P) + C_2D_2 reaction obtained by theory and molecular beam experiments (straight line and normalized to the theoretical result at an energy of 1 kJ mol^{-1}) plotted against the logarithm of the collisional energy.

results, described in section III, for the C(^{3}P) + C_2D_2 reaction. Special attention to the numerical aspects of the wave packet results has enabled converged cross sections to be obtained for lower energies than reported previously.[28] It can be seen from Figure 16 that the agreement between theory and experiment is quite good, and the sharp increase with the cross section as the energy is decreased is observed. It is interesting to point out that some ab initio calculations predict that the linear C_3D isomer is not thermodynamically allowed at lower collision energies for this reaction,[19,38] but this does not seem to influence the energy dependence of the experimentally observed integral cross sections (see section III.2).

VI. Conclusions

The reaction of C(^{3}P) with acetylene is an important reaction in dense interstellar clouds. As the potential energy surface is barrierless, the rate constant is large, even at very low temperatures. As products such as C_3H can be formed, the reaction is a first step in the synthesis of larger carbon chain molecules. Advances in experiment and theory make this a prototype reaction for detailed study using the latest methods of reaction dynamics and computation.

This feature article has brought together some of the recent work that has been done to understand the detailed mechanism of the reaction. The kinetic experiments performed in Birmingham have shown that the reaction rate constant remains large down to 15 K and is almost temperature independent between 15 and 300 K. The latest theory carried out in London, that exploits first principles electronic structure calculations and wave packet dynamics, gives absolute rate constants in quite good agreement with the experiments except at very low temperatures where a rise in the rate constant with increasing temperature is predicted. Molecular beam experiments on the C(^{3}P) + C_2H_2 and C_2D_2 reactions performed in Bordeaux give an energy dependence of the integral cross sections that is in accord with the kinetic experiments and the wave packet calculations. These results confirm unequivocally that there is no barrier or effective barrier in the potential energy surface for the reaction.

There is particular interest in the products of the reaction as both linear and cyclic C_3H can be formed, together with C_3 + H_2. Because the two isomers of C_3H have been detected with high abundances in the interstellar medium,[21] and in varying proportions depending on the interstellar source, it is of particular interest to determine the branching ratio for their formation. This has not yet been achieved experimentally, although some mechanistic information has been inferred from crossed molecular beam differential cross section measurements. An interesting prediction from the wave packet calculations is that production of linear C_3H is preferred over the cyclic isomer at lower collision energies. However, this result is based on several approximations, and a detailed dynamics study that treats all degrees of freedom from reactants to products on an accurate potential surface is needed to confirm the prediction. A particularly novel finding in the crossed molecular beam experiments, which are described here in section IV, is that the C_3 + H_2 product can also be formed. This requires an intersystem crossing mechanism. This result also has implications for understanding interstellar chemistry as C_3 has been detected in various astrophysical environments.[22−24]

It is clear from the work described here on the C(^{3}P) + C_2H_2 reaction that modern reaction dynamics methods have useful applications and provide detailed information that cannot be obtained by other techniques. The experimental results require detailed theory for their interpretation, using the best electronic structure and dynamics methods. However, despite the considerable amount of work that has been done, there remain many unanswered questions concerning this prototypical organic reaction that might have seemed simple at a first consideration. In particular, a complete understanding of the product branching ratios of the reaction will only come from the continued development and application of new techniques in reaction dynamics, stimulated by the need for detailed data from fields such as astrophysics.

Acknowledgment. This work in Birmingham, Bordeaux, Perugia and London was supported by a TMR Research Network grant of the European Union, "Astrophysical chemistry: Experiments, calculations and astrophysical consequences of reactions at low temperatures" under Contract FMRX-CT97-0132 (DG12-MIHT). The authors in Bordeaux acknowledge the financial support from the Conseil Régional d'Aquitaine and the Program National Physique du Chimie du Milieu Interstellaire. Support of the work in Perugia by the "Ministero Università e Ricerca Scientifica (MURST)" is gratefully acknowledged. The authors in Birmingham acknowledge the contribution of Dr. Delphine Chastaing and Dr. Sebastien Le Picard in performing the experimental kinetic investigations

reported here, and the authors from Perugia acknowledge the contribution from Giovanni Capozza and Astrid Bergeat. The work in London and Birmingham was also supported by the Engineering and Physical Sciences Research Council.

References and Notes

(1) Cardelli, J. A.; Meyer, D. M.; Jura, M.; Savage, B. D. *Astrophys. J.* **1996**, *467*, 334.
(2) Bell, M. B.; Feldman, P. A.; Travers, M. J.; McCarthy, M. C.; Gottlieb, C. A.; Thaddeus, P. *Astrophys. J.* **1997**, *483*, L61.
(3) Smith, I. W. M.; Rowe, B. R. *Acc. Chem. Res.* **2000**, *33*, 261.
(4) Sims, I. R.; Smith, I. W. M. *Annu. Rev. Phys. Chem.* **1995**, *46*, 109.
(5) Herbst, E.; Lee, H. H.; Howe, D. A.; Millar, T. J. *Mon. Not. R. Astron. Soc.* **1994**, *268*, 335.
(6) Herbst, E. *Chem. Soc. Rev.* **2001**, *30*, 168.
(7) Herbst, E. *Annu. Rev. Phys. Chem.* **1995**, *46*, 27.
(8) Phillips, T. G.; Huggins, P. J. *Astrophys. J.* **1981**, *251*, 533.
(9) Zmuidzinas, J.; Betz, A. L.; Boreiko, R. T.; Goldhaber, D. M. *Astrophys. J.* **1988**, *335*, 774.
(10) Evans, N. J.; Lacy, J. H.; Carr, J. S. *Astrophys. J.* **1991**, *383*, 674. Schilke, P.; Keene, J.; Lebourlot, J.; Desforets, G. P.; Roueff, E. *Astron. Astrophys.* **1995**, *294*, L17.
(11) Haider, N.; Husain, D. *J. Chem. Soc., Faraday Trans.* **1993**, *89*, 7.
(12) Clary, D. C.; Haider, N.; Husain, D.; Kabir, M. *Astrophys. J.* **1994**, *422*, 416.
(13) Smith, D.; Adams N. G. *Int. Rev. Phys. Chem.* **1981**, *1*, 171.
(14) Chastaing, D.; James, P. L.; Sims, I. R.; Smith, I. W. M. *Phys. Chem. Chem. Phys.* **1999**, *1*, 2247.
(15) Geppert, W. D.; Reignier, D.; Stoecklin, T.; Naulin, C.; Costes, M.; Chastaing, D.; Le Picard, S. D.; Sims, I. R.; Smith, I. W. M. *Phys. Chem. Chem. Phys.* **2000**, *2*, 2873. Chastaing, D.; Le Picard, S. D.; Sims, I. R.; Smith, I. W. M.; Geppert, W. D.; Naulin, C.; Costes, M. *Chem. Phys. Lett.* **2000**, *331*, 170.
(16) Chastaing, D.; Le Picard, S. D.; Sims, I. R. *J. Chem. Phys.* **2000**, *112*, 8466.
(17) Chastaing, D.; Le Picard, S. D.; Sims, I. R.; Smith, I. W. M. *Astron. Astrophys.* **2001**, *365*, 241.
(18) Kaiser, R. I.; Stranges, D.; Lee, Y. T.; Suits, A. G. *Astrophys. J.* **1997**, *477*, 982.
(19) Kaiser, R. I.; Ochsenfeld, C.; Head-Gordon, M.; Lee, Y. T.; Suits, A. G. *J. Chem. Phys.* **1997**, *106*, 1729. Ochsenfeld, C.; Kaiser, R. I.; Lee, Y. T.; Suits, A. G.; Head-Gordon, M. *J. Chem. Phys.* **1997**, *106*, 4141.
(20) The exoergicity is obtained by using $\Delta_f H_0^0(C(^3P)) = 711.2$ kJ mol^{-1} (*Handbook of Chemistry and Physics*; CRC Press: Boca Raton, FL, 1999−2000), $\Delta_f H_0^0(C_2H_2) = 227.3$ kJ mol^{-1} (Okabe, H. *Photochemistry of Small Molecules*; Wiley: NewYork, 1972), and $\Delta_f H_0^0(C_3) = 833.9$ kJ mol^{-1} (Gingerich, K. A.; Finkbeiner, H. C.; Schmude, R. W., Jr. *J. Am. Chem. Soc.* **1994**, *116*, 3884).
(21) Turner, B. E.; Herbst, E.; Terzieva, R. *Astrophys. J. Suppl. Ser.* **2000**, *126*, 427.
(22) Hinkle, K. W.; Keady, J. J.; Bernath, P. F. *Science* **1988**, *241*, 1319.
(23) Bernath, P. F. Laboratory Astrophysics and Molecular Astronomy of Pure Carbon Molecules. In *Life Sciences and Space Research XXV (4)*; Pergamon Press Ltd: Oxford, U.K., 1994; Vol. 15, p 15.
(24) Cernicharo, J.; Goicoechea, J. R.; Caux, E. *Astrophys. J.* **2000**, *534*, L199.
(25) Takahashi, J.; Yashimata, K. *J. Chem. Phys.* **1996**, *104*, 6613.
(26) Guadagnini, R.; Schatz, G. C.; Walch, S. P. *J. Phys. Chem. A* **1998**, *102*, 5857.
(27) Mebel, A. M.; Jackson, W. M.; Chang, A. H. H.; Lin, S. H. *J. Am. Chem. Soc.* **1998**, *120*, 5751.
(28) Buonomo, E.; Clary, D. C. *J. Phys. Chem. A* **2001**, *105*, 2694.
(29) Naulin, C.; Costes, M. *Chem. Phys. Lett.* **1999**, *310*, 231.
(30) Geppert, W. D.; Naulin, C.; Costes, M. *Chem. Phys. Lett.* **2001**, *333*, 51.
(31) Bergeat, A.; Loison, J. C. *Phys. Chem. Chem. Phys.* **2001**, *3*, 2038.
(32) Reid, A. S.; Winterbottom, F.; Scott, D. C.; de Huan, J.; Reisler, H. *Chem. Phys. Lett.* **1992**, *198*, 430.
(33) Casavecchia, P. *Rep. Prog. Phys.* **2000**, *63*, 355.
(34) Casavecchia, P.; Balucani, N.; Cartechini, L.; Capozza, G.; Bergeat, A.; Volpi, G. G. *Faraday Discuss.* **2001**, *119*, 27.
(35) James, P. L.; Sims, I. R.; Smith, I. W. M.; Alexander, M. H.; Yang, M. B. *J. Chem. Phys.* **1998**, *109*, 3882.
(36) Haider, N.; Husain, D. *J. Photochem. Photobiol. A* **1993**, *70*, 119.
(37) Kaiser, R. I.; Lee, Y. T.; Suits, A. G. *J. Chem. Phys.* **1995**, *103*, 10395.
(38) Kaiser, R. I.; Ochsenfeld, C.; Head-Gordon, M.; Lee, Y. T.; Suits, A. G. *Science* **1996**, *274*, 1508. Kaiser, R. I.; Ochsenfeld, C.; Head-Gordon, M.; Lee, Y. T. *Astrophys. J.* **1999**, *510*, 784.
(39) Wilson, S. H. S.; Reed, C. I.; Mordaunt, D. H.; Ashfold, M. N. R.; Kawasaki, M. *Bull. Chem. Soc. Jpn.* **1996**, *69*, 71.
(40) Ohishi, M.; Kaifu, N. *Faraday Discuss.* **1998**, *109*, 205.
(41) Giesen, T. F.; Van Orden, A. O.; Cruzan, J. D. *Astrophys. J.* **2001**, *551*, L181.
(42) Churyumov, K. I.; Kleshchonok, V. V.; Kravtsov, F. I. *Planet. Space Sci.* **1994**, *42*, 737.
(43) Seburg, R. A.; Patterson, E. V.; Stants, J. F; McMahon, R. J. *J. Am. Chem. Soc.* **1997**, *119*, 5847.
(44) Alagia, M.; Balucani, N.; Casavecchia, P.; Stranges, D.; Volpi, G. G. *J. Chem. Soc., Faraday Trans.* **1995**, *91*, 575.
(45) Bergeat, A.; Cartechini, L.; Balucani, N.; Capozza, G.; Phillips, L. F.; Casavecchia, P.; Volpi, G. G.; Bonnet, L.; Rayez, J.-C. *Chem. Phys. Lett.* **2000**, *327*, 197.
(46) Jackson, W. M.; Anex, D. S.; Continetti, R. E.; Lee, Y. T. *J. Chem. Phys.* **1991**, *95*, 7327.
(47) Kaiser, R. I.; Le, T. N.; Nguyen, T. L.; Mebel, A. M.; Balucani, N.; Lee, Y. T.; Stahl, F.; Schleyer, P.v. R.; Schaefer, H. F., III. *Faraday Discuss.* **2001**, *119*, 50.
(48) Dunning, T. H. *J. Chem. Phys.* **1989**, *90*, 1007.
(49) Zhang, D. H.; Zhang, J. Z. H. *J. Chem. Phys.* **1994**, *101*, 3671.
(50) Light, J. C.; Hamilton, I. P.; Lill, J. V. *J. Chem. Phys.* **1985**, *82*, 1400.
(51) Vibok, A.; Balint-Kurti, G. G. *J. Phys. Chem.* **1992**, *96*, 8712.
(52) Clary, D. C. *Mol. Phys.* **1985**, *54*, 605.